# In-silico and in-vitro study reveals Ziprasidone as a potential aromatase inhibitor against breast carcinoma

ankita sahu[1], Shaban Ahmad[2], Khalid Imtiyaz[3], Mojahidul Islam[4], Khalid Raza[2], Murugesh Easwaran[5], Moshahid Rizvi[3], and Saurabh Verma[1]

[1]National Institute of Pathology
[2]Jamia Millia Islamia Department of Computer Science
[3]Jamia Millia Islamia Central University
[4]Institute of Liver and Biliary Sciences
[5]International Centre for Genetic Engineering and Biotechnology New Delhi

September 26, 2022

**Abstract**

Background and Purpose: The aromatase enzyme plays a fundamental role in addressing the development of estrogen receptors and giving attention to the therapy of reproductive disorders and cancer diseases. In clinical use, the objectionable effects found in these target inhibitors are indispensable in finding novel aromatase inhibitors with more selective, less toxic, and more effective drug potency. Experimental Approach: The research framework of this study is to identify a potent inhibitor for the aromatase target by profiling molecular descriptors of the ligand and finding a functional pocket of the target by docking and MD simulations. For assessing cellular metabolic activities as an indicator of cell viability and cytotoxicity, in-vitro studies were performed by using colorimetric MTT assay. Cell morphology was assessed by phase-contrast light microscope. Cell cycle distribution and apoptosis were determined by flowcytometry and Annexin V-FITC/PI staining assay. Key Results: This study reported herein the most promising compound CHEMBL598797 (Ziprasidone) showed excellent activity potential to inhibit aromatase in search of finding the novel compound based on better drug design methods and experimental studies and could be effective as the high potential drug candidate against aromatase enzyme. Conclusion and Implications: We concluded that the compound ziprasidone effectively blocks the cell cycle at the G1-S phase and induces cancer cell death. Further in-vivo studies can be evaluated for developing this compound as an anticancer agent. Overall, our outcomes based on the in-silico and the high-quality experimental results may pave the way for identifying effective drug candidates for better therapeutic interest for breast cancer.

# *In-silico* and *in-vitro* study reveals Ziprasidone as a potential aromatase inhibitor against breast carcinoma

**Ankita Sahu[1], Shaban Ahmad[2], Khalid Imtiyaz[3], Mojahidul Islam[4], Khalid Raza[2*], Murugesh Easwaran[5], Moshahid A. Rizvi[3], Saurabh Verma[1#]**

[1]Tumour Biology, ICMR-National Institute of Pathology, New Delhi, India-110029
[2]Department of Computer Science, Jamia Millia Islamia -110025
[3]Department of Bioscience, Jamia Millia Islamia, New Delhi, India-110025
[4]Molecular and Cellular Medicine, Institute of Liver and Biliary Sciences, Delhi, India-110070
[5]Nutritional Improvement of Crops, Plant Molecular Biology Division, International Centre of Genetic Engineering and Biotechnology, New Delhi, India-110067

*Co-Authors
Ankita Sahu: Ankitasahumbt@gmail.com (ORCID ID: 0000-0001-6679-3486)
Shaban Ahmad: Shaban184343@st.jmi.ac.in (ORCID ID: 0000-0001-9832-2830)
Khalid Imtiyaz: Khaliddar123@gmail.com (ORCID ID: 0000-0003-2854-5857)
Mojahidul Islam: Islammojahidul4@gmail.com (ORCID ID: 0000-0001-7219-9686)
Khalid Raza: Kraza@jmi.ac.in (ORCID ID: 0000-0002-3646-6828)
Murugesh Easwaran: Murugeshphdsch@gmail.com (ORCID ID: /0000-0001-7628-0772)
Moshahid A. Rizvi: mrizvi@jmi.ac.in (ORCID ID: 0000-0002-4449-7819)

**[#]Corresponding Author**
**Dr Saurabh Verma**
Tumour Biology, ICMR-National Institute of Pathology, New Delhi, India-110029
**Contact:** svarmasv1@rediffmail.com, /saurabhverma.nip@gov.in
ORCID ID: 0000-0003-1489-1871

***Co-Corresponding Author**
**Dr Khalid Raza**
Department of Computer Science, Jamia Millia Islamia -110025
**Contact:** Kraza@jmi.ac.in
ORCID ID: 0000-0002-3646-6828

**Abstract:**

**Background and Purpose:** The aromatase enzyme plays a fundamental role in addressing the development of estrogen receptors and giving attention to the therapy of reproductive disorders and cancer diseases. In clinical use, the objectionable effects found in these target inhibitors are indispensable in finding novel aromatase inhibitors with more selective, less toxic, and more effective drug potency.

**Experimental Approach:** The research framework of this study is to identify a potent inhibitor for the aromatase target by profiling molecular descriptors of the ligand and finding a functional pocket of the target by docking and MD simulations. For assessing cellular metabolic activities as an indicator of cell viability and cytotoxicity, *in-vitro* studies were performed by using colorimetric MTT assay. Cell morphology was assessed by phase-contrast light microscope. Cell cycle distribution and apoptosis were determined by flowcytometry and Annexin V-FITC/PI staining assay.

**Key Results:** This study reported herein the most promising compound CHEMBL598797 (Ziprasidone) showed excellent activity potential to inhibit aromatase in search of finding the novel compound based on better drug design methods and experimental studies and could be effective as the high potential drug candidate against aromatase enzyme.

**Conclusion and Implications:** We concluded that the compound ziprasidone effectively blocks the cell cycle at the G1-S phase and induces cancer cell death. Further *in-vivo* studies can be evaluated for developing this compound as an anticancer agent. Overall, our outcomes based on the in-silico and the high-quality experimental results may pave the way for identifying effective drug candidates for better therapeutic interest for breast cancer.

**Keywords:** Aromatase, Molecular docking, Molecular Dynamics simulation, MTT assay, Apoptosis.

## 1. Introduction:

Breast cancer (BC) is an utmost form of cancer globally, reported primarily in females (>99%) and very rarely in males (<1%) population. The development and progression of breast carcinoma depend on genetic abnormality and hormonal deregulation (Smith and Dowsett, 2003). The worldwide incidence of BC is 25 % of all cancers in women. In regions of lesser economic status, it is women's most common cause of death. The incidence of breast cancer is most common after menopause (World Cancer Research Federation WCRF (https://www.wcrf.org/dietandcancer/breast-cancer). Numerous pathophysiological reasons like gene mutations (especially breast cancer gene BRAC1 and BRAC2), inherited genetic predisposition, exposure to the hormone (estrogen and progesterone), diet-related, and environmental/lifestyle exposures lead to breast cancer development (Michels, 2002; Travis and Key, 2003). Several potential targets, such as vascular endothelial growth factor, epidermal growth factor receptor, and tremendous enzymes, were reported to identify cancers and reproductive diseases (Atalay et al., 2003; Arora and Scholar, 2005; Appert-Collin et al., 2015).

Aromatase hemo protein-containing enzymatic complex in the endoplasmic reticulum of estrogen-producing cells, also known as Cytochrome P450 19A1, comprises a prosthetic heme group and a polypeptide chain of 503 residues (Shaheenah et al., 2008; Kumavath et al., 2016). It consists of 9 exons and a 5′-untranslated region on the human CYP19 gene (localisation of 15q21.1 region), stretching ~123 kb. It catalyses the conversion of androgens precursors to aromatic estrogens (Anthoni et al., 2012; Lephart, 2015). The aromatase enzyme does this conversion, becoming a promising target that addresses reproductive disorders and malignancies (Mori et al., 2018). The transformation occurs in the androgen-specific cleft containing polar hydrophobic residues that stimulate cellular proliferation in breast cancer (Altundag and Ibrahim, 2006; Lephart, 2015). This reaction oxidises and subsequently removes the methyl group at the A ring to bring it into an aromatic state, thus converting androgen into

estrogen (Lephart, 2015). Estrogen surge in the breast tissues is the primary hormonal requirement for the progression of tumorigenesis.

Aromatase is a rate-limiting enzyme found in several human tissues subcutaneous fat, placental syncytiotrophoblasts, ovarian granulosa cells, skin fibroblasts, adipose tissue, osteoblasts of bone, brain and cancerous as well as normal breast tissues (Nelson and Bulun, 2001; Czajka-Oraniec and Simpson, 2010; Mori et al., 2018). The source of residual estrogen is solely non-glandular especially subcutaneous fat. The estradiol level in breast carcinoma tissues is several times higher than in the blood because of its overexpression in such tissues (Travis and Key, 2003; Chan et al., 2016). This increases the significance of therapeutic monomeric aromatase enzyme inhibition as a front-line therapeutic intervention in estrogen hormone-dependent breast cancer. Only influential post-menopausal women (Altundag and Ibrahim, 2006; Santen et al., 2009) have less effectiveness in inhibiting ovarian peripheral estrogen formation or local estrogen production. Consequently, they are most frequently used to inhibit tumour growth and breast cancer cell proliferation.

A drug discovery process originates with some clinical conditions to find suitable pharmaceutical drugs. The initial step of the research process starts via bioinformatics analysis with the identification and validation of biological targets (Cava and Castiglioni, 2020) that cover the biological entities, including protein, gene and RNA, which can be quantified by the experimental method *in-vitro* and *in-vivo* models. The protein's functioning can be studied at the atomic level using different techniques and algorithms for molecular docking, ADMET profile, and simulation of their three-dimensional structures. The development of new compounds for the inhibition of aromatase enzymes is essential for biomedicinally drug designing. Herein, we selected the compound from ChEMBL databases as a vital source for drug discovery in the biological system. The biocomputational tools are the key technology for computational biology and health informatics to develop lead compounds (Davies et al., 2015).

The selecting appropriate protein structures and searchable drug databases requires molecular docking strategies to find biological and chemical features. It is widely known that *in-silico*-based docking studies, residue-protein interaction patterns, ADMET properties, and MD simulation help identify the appropriate drugs/molecules to avoid the time, cost, and adverse consequences of preclinical studies (Paul et al., 2010). Thus, high-performing computational algorithms for the drug design process are required. Molecular docking and MD simulation strategies were used to identify a potent inhibitor of the aromatase target.

This study aims to identify aromatase inhibitors using an *in-silico* approach. This research will be outlined from the ChEMBL database screening with the aromatase target protein and explore the various *in-silico* strategies for regulating the biological processes involved in breast cancer progression to find a better outcome. Then, the study was extended to validate the compound in *in-vitro* conditions.

## 2. Materials and Methods:

Our studies are comprised of a regress in-silico analysis and in-vitro analysis. The in-silico analysis that are from data collection, preparation and validation, molecular docking, MM\GBSA, molecular dynamics simulation and ADMET analysis. At the same time, the in-vitro analyses are cell culture and drug treatment, cell proliferation assay, cell cycle analysis, and Annexin V-FITC/PI staining assay for Apoptosis. A graphical abstract represents to understand the complete methods.

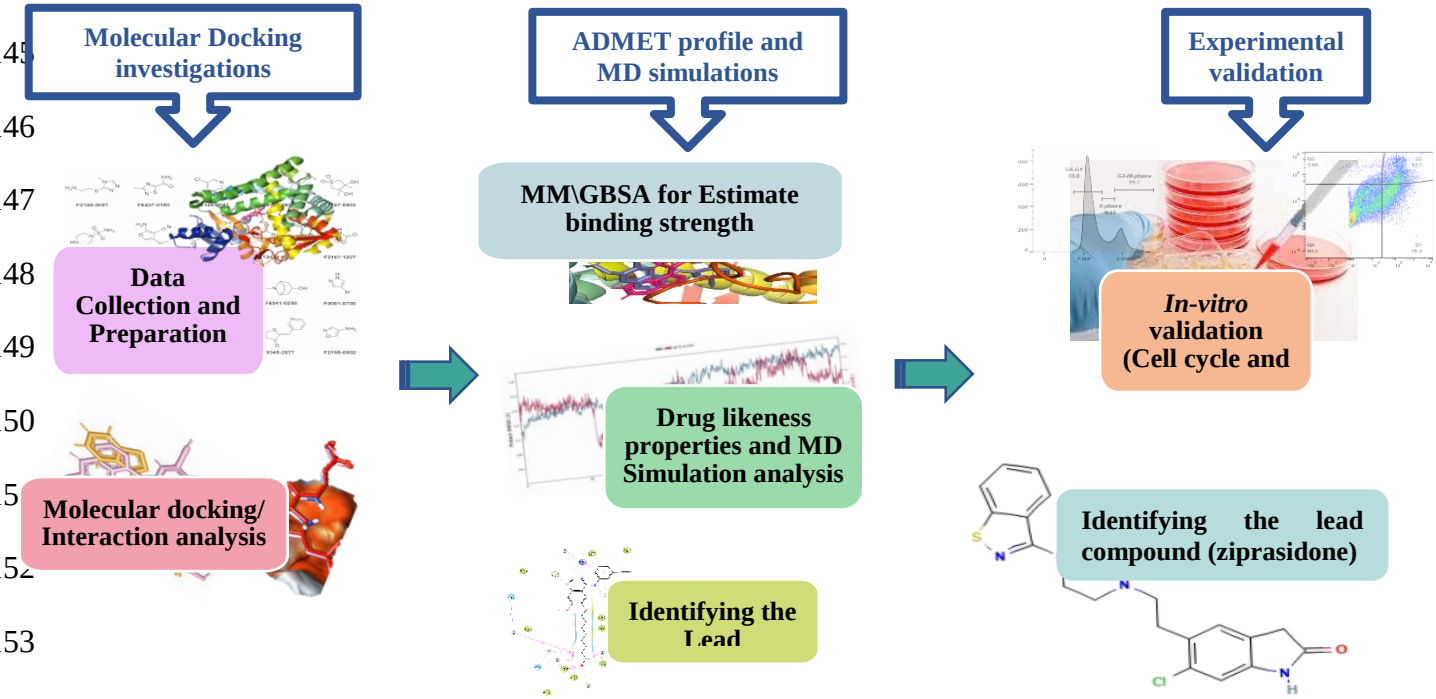


***Graphical abstract of the complete computer-aided drug discovery and in vitro approaches***

## 2.1 Protein Structure Prediction and Validation:

Numerous experimental structures are discovered in the protein data bank (PDB). The best matching structure of aromatase enzyme was chosen from the RCSB PDB, freely available at www.rcsb.org (Berman et al., 2000), based on the different parameters such as resolution, organism(s), methods (x-ray crystallographic structure, EM structure), mutation and other features. A three-dimensional structure of aromatase target protein (PDB ID 3EQM) defined as a target was selected, which contains Cytochrome P450 19A1 with X-ray diffraction 2.9Å resolution, and the sequence length consists of 503 amino acid residues. The structure was optimised, and energy minimisation was performed by default constraint of 0.3 A of Root mean Standard Deviation (RMSD) with OPLS force field using Macro model, Schrodinger suite, LLC, New York, NY, 2015. Added hydrogen atoms to the targeted protein to retain the tautomeric states and stabilise the ionisation of amino acid residues (Sastry et al., 2013). The PROCHECK Ramachandran Plot server was applied to analyse the geometry of the amino acids in the target protein, the conformation of the residual angle, and the interactions between

the atoms (Laskowski et al., 1993; Sahu et al., 2017) and the prepared protein is shown in Figure 1.

### 2.2 Database preparation for bioactive conformation:

Database preparation is crucial to finding the lead compound in the screening campaign. Researchers have constructed many drugs-like compounds library from the large-scale bioactivity database ChEMBL (https://www.ebi.ac.uk/chembl/). This library of the ligands is a dictionary of small molecule entities with over 2 million compounds recorded. The LigPrep (Schrodinger suite 2015) module was used for ligand preparation to assign the protonation states at biologically relevant pH. We prepared the library of 8506 compounds from the ChEMBL version 26 database, representing a significant source of chemical and biological information such as binding, functional, cellular activity, and ADMET data (Gaulton et al., 2012; Davies et al., 2015). The library was downloaded in SDF format.

### 2.3 Active Site Prediction:

The binding site of the amino acids is required for further molecular docking studies (Ghosh et al., 2010). The protein's active site was determined using Schrodinger's Sitemap Programme (Friesner et al., 2004). Specific interaction of aromatase protein with five top-ranking surface pockets was identified as a suitable binding site responsible for its drug-like compound cavity. The site with a Site score close to one was chosen for grid generation. The grid was generated using Glide v6.6, Schrodinger 2015. 3.1.

### 2.4 Molecular docking:

Docking experiments were conducted on Glide XP (extra precision) docking mode v6.6 module (Friesner et al., 2004, 2006; Ferreira et al., 2015) and the molecular mechanics\ Generalized Born Surface Area (MM\GBSA) (Genheden and Ryde, 2015; Wang et al., 2019) for the interaction of suitable complex of receptor-ligand structure has been calculated via post docking analysis called Prime in v3.6 Schrodinger Suite 2020. The ligand docking protocol

examined the compound's crucial phase of binding free energies (Alonso et al., 2006; Torres et al., 2019). It determines whether a combination will bind or separate from the protein surface and return to its unbound state (Elokely and Doerksen, 2013; Torres et al., 2019). The docked complex was performed by evaluating the hydrogen bond interaction, hydrophobic interaction, pi-pi interaction, and pi cation interaction in Schrodinger software.

Additionally, the docked complex was refined to calculate ΔG from MM-GBSA analysis (Zhang et al., 2017). The "MMGBSA Δ*G* Bind" calculation [*dG*(1)] was done by following an equation:

*dG(1) = E_complex (minimized) - (E_ligand (minimized) + E_receptor (minimized))*

where the formula of MMGBSA designates molecular mechanics energies combined with the generalized Born and surface area continuum solvation; *dG* bind denotes the computed free energy of ligand and receptor; *E_complex* is the MM/GBSA energy of the minimized complex, *E_receptor* represents MM/GBSA energy of protein (unbound, minimized) without ligand and *E_ligand* denotes the MM/GBSA energy of the ligand after removing it from the complex. We obtained reliable top compounds based on docking score, MM-GBSA, and Qikprop module. The results are given in Table 1 and Table 2. Further, molecular dynamic simulation was performed on docked protein-ligand complex.

### 2.5 ADMET investigation:

ADME/Tox studies continue to drive the success of biological functions for creating a target for drug candidates. There are many reasons to estimate that 50% of drug candidates fail to win approval due to the lack of potential efficacious and that up to 40% of drug candidates have failed in the past due to toxicity. The analytical software Qikprep module from Schrodinger suite 2020 was used for predicting the pre-assessing the Adsorption, Distribution, Metabolism, and Elimination (ADME) properties which provide some important information related to the drugs/molecules. All compounds were calculated using QikProp 3.4 modules to identify promising molecules that follow the bioavailability characteristics and ADMET

profiling (Norinder and Bergström, 2006; Cheng et al., 2013). The criteria for ADME properties include SASA, FOSA, and FISA. Acceptable ranges are 300-1000, 0-750, and 7-330, respectively (Dasari et al., 2017), total solvent-accessible volume range from 500-2000; QPlogKhsa favourable range -1.5−1.5; molecular weight (mol MW) less than 500; Hydrogen bond donor and acceptor with the range of 0.0-6.0 and 2.0-20.0; QPlogHERG with an acceptable range less than<-5; QPPMDCK with the normal range nm per sec. greater than 500; QPlogPC16 which used for projected the hexadecane/gas partition coefficient recommended range 4.0-18.0; octanol/water partition coefficient (QPlogPo/w) acceptable range is 3.069-3.905, QPlogPoct acceptable range is 8.0-35.0 (octanol/gas); QPlogKp with the normal range from -8 to -10; QPlogPw (water/gas) with favourable range 4.0-45.0; QPlogBB and QPPCaCo with normal range -3−1.2 and (>500) (Egan and Lauri, 2002; Ntie-Kang, 2013; Shahbazi et al., 2016).

**2.6 Molecular Dynamic Simulation:**

Molecular dynamics are now routinely applied to investigating dynamic properties and processes in several areas of structural biochemistry, pharmaceutical chemistry, Molecular biology, enzymology, biophysics, and biotechnology. It is an invaluable tool extensively used to study the protein's biomolecule structure-function correlation (Rana et al., 2021). It allows a comprehensive of several dynamic biomolecular structures' characteristics, recognition, and function. (Karplus and McCammon, 2002; Adcock and McCammon, 2006; Alonso et al., 2006). The molecular dynamics trajectory represents the computer simulation method for molecular systems, which provides the atomic coordinates at a specific period, single-point energies, and velocities (Adcock and McCammon, 2006). Several algorithms exist for running MD simulations under different criteria (Alonso et al., 2006; Sahu et al., 2020). MD simulation was performed using the Desmond *v3.6* package from Schrodinger. Figure 3 and Figure 4 illustrate the high density at the centre of an orthorhombic box with the periodic frontier

condition. This module helps determine the RMSD value, Protein-Ligand torsion, protein-ligand interaction, validation, and optimisation. Simulation time was set up to 100 ns with a trajectories recording at each 100 ps interval and an orthorhombic box with TIP3P. The water molecule was set up to specify the shape. The system was further neutralised by adding the system charge $Na^+$ ion. Temperature and pressure on the Kalvin scale were constant at 300 K in the equilibration period and 1.01325 bar, respectively (Alonso et al., 2006). Obtained trajectories were then analysed using Simulation Interaction Diagram.

### 2.7 Biological evaluation (*In-vitro* studies):

Based on the *in-silico* studies, we found the commercially available lead compound ziprasidone. This compound was selected for our in-vitro experimental studies.

#### 2.7.1 Cell culture and drug treatment:

Human breast (MCF-7, MDA-MB-231 and T47D) cancer cells were procured from National Centre for Cell Sciences (NCCS), Pune, India. The cells were maintained in Dulbecco's Modified Eagle's medium (HiMedia, Mumbai) with 10% FBS (HiMedia, Mumbai), 100 U/mL penicillin, 100 mg/mL streptomycin and 250 ng/mL amphotericin B at 37$^o$C in a humidified chamber consisting 5% $CO_2$ and 95% air. Cells were then incubated with standard trypsinisation (Trypsin: 0.25%) at 85% confluency and subcultured in a ¼ ratio for routine maintenance and experimentation. Compound ziprasidone was prepared in DMSO and exposed to the cells for 24h and 48h at a final volume of 0.1% DMSO.

#### 2.7.2 Cell proliferation assay:

The inhibitory effect of selected drugs was measured by MTT assay. Different breast cancer cell lines such as MCF-7, MDA-MB-231 and T47D were grown overnight in 96 healthy ELISA plates at a density of 8 x 10 3 cells/well and treated with a drug from 0.62 mM to 2 mM for 24h and 48h. MTT (5mg/ml) was added at the end of incubation for 3-4h. Afterwards, the

medium was removed, dimethyl sulfoxide (100 µL/well) was added, and incubated for 5min at 37$^{o}$C under shaking conditions. Absorbance values at 570 nm were recorded using an ELISA plate reader, and the $IC_{50}$ value was calculated from the dose-response curve.

### 2.7.3 Cell cycle analysis:

Cell cycle progression was evaluated using a Flowcytometry. MCF-7, MBA MD 231, and T47D human breast cancer cells were incubated for 48 h with the compound ziprasidone at IC50 value obtained by MTT assay. After 48 h of treatment, cells were harvested, washed twice with PBS, and fixed in ice-cold 70% ethanol overnight at 4℃. Next day, all samples were centrifuged at 3000 rpm for 4 min. The cells were counterstained with propidium iodide (5mg/ml) followed by addition of RNase and acquired on a spectrum flow cytometer (Cytek Aurora, Cytek Biosciences, Fremont, CA, USA) and DNA content was measured under blue laser (488nm) and a complete spectrum was captured in all 14 channels (B1-B14). The maxima was attained at 615/20 nm filter (B6). Data analysis was done by FlowJo software Version 10.8.1 (BD Biosciences, Ashland, OR, USA).

### 2.7.4 Annexin V/PI staining assay for Apoptosis:

Human breast cancer cell lines (MCF-7, MDA MB 231, and T47D) cells were seeded in 6-well plates at 10 x10 and 4 cells per well and grown overnight. Then cells were treated for 48 h with compound at IC50 value obtained by cell viability assay. After 48 h, cells were trypsinised, washed with Phosphate-buffered saline (PBS), and stained with annexin V-fluorescein isothiocyanate (FITC) and propidium iodide (PI) from Alexa Fluor 488 annexin V apoptosis detection kit (Beckman Coulter) using manufacturer protocol, followed by acquisition on a spectrum flow cytometer (Cytek Aurora, Cytek Biosciences, Fremont, CA, USA). Data analysis was done by FlowJo software Version 10.8.1 (BD Biosciences, Ashland, OR, USA).

## 3. Results and discussion:

### 3.1 *In-silico* studies:

#### 3.1.1 3D-structure modelling and validation:

Ramachandran plot for the selected structures was downloaded for this structure, assessing the stereochemical quality of the protein structure. By using the PROCHECK server, as shown in Figure 1(B). Residues in the beta-conformation are negative, followed by 0 to -60 psi angles (ψ) and 0 to -90 in the phi angles (ϕ) are positive, showing dense conformation of residues in the targeted aromatase protein. Based on the results, 94.33% residues were found in the most favoured region, 4.67% amino acid residues were likely found in the additional allowed region, 1% in the generously disallowed area and none of the residue (white region) in the disallowed region.

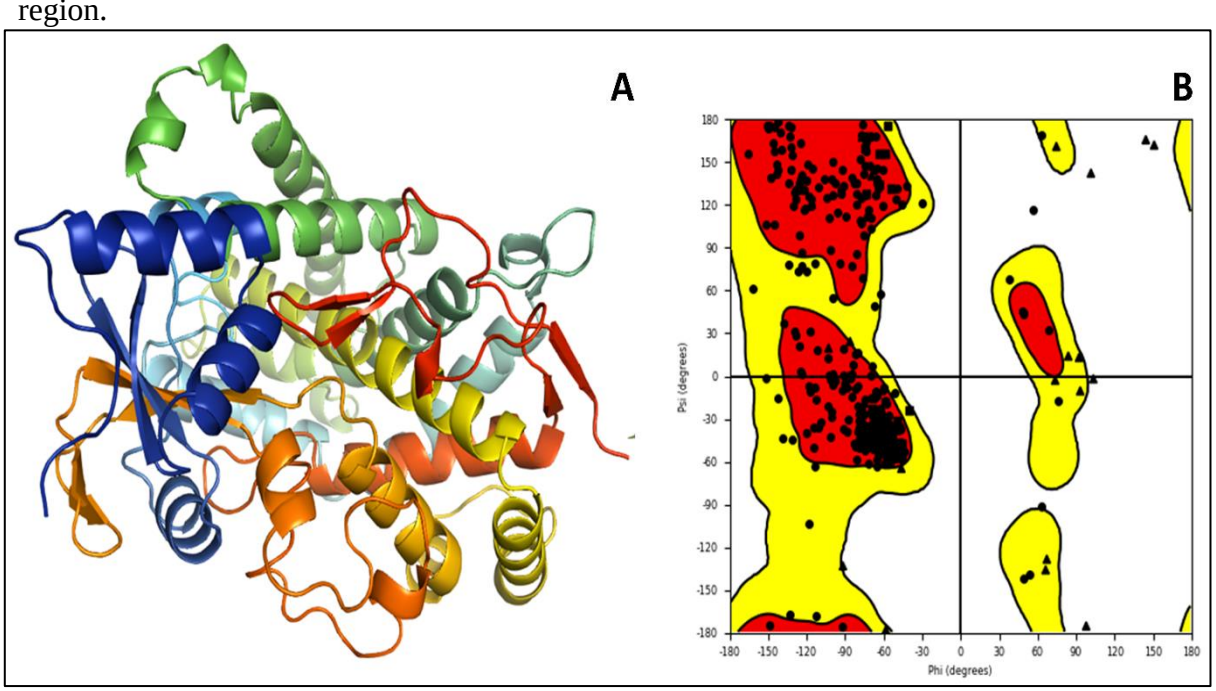


**Figure 1: A)** 3D Crystal structure of aromatase (PDB ID:3EQM), and **B)** Ramachandran plot of prepared structure

#### 3.1.2 Binding affinity calculation:

The bound structure of receptors with ligands is considered a therapeutic target for breast cancer treatment and screened out with the ChEMBL database by a molecular docking study. The docking calculation details the binding energies between the selected drugs and the carrier systems. The GlidScore was analysed, and the top-ranked compound was found through

docking results. The attractive force and binding affinity of interacting protein-ligand docked structure determine the binding affinity. The binding affinity values for the docked structure of aromatase protein are displayed in Table 1. The lowest Glide Score characterises the more agreeable binding. In the binding site, the binding conformation of the aromatase receptor is supposed to a purpose for their remarkable inhibitory effect against aromatase activity shown in Figure 2. Further, the MM\GBSA calculated for binding free energy score with OPLS-2005 gives a much more accurate scoring of the ligand pose than the XP score. The scoring was observed to be more effective in the ranking ligand; compound CHEMBL598797 shows good aromatase inhibiting tendency with $\Delta G_{MM\text{-}GBSA}$ values of -88.31 kcal/mol, respectively.

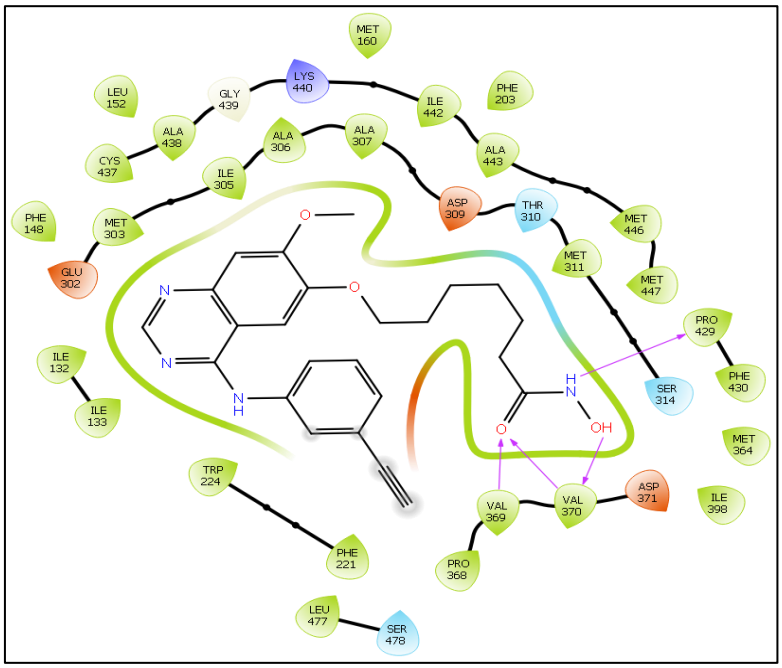


**Figure 2.** Showing the ligand interaction diagram of the 3EQM and Ziprasidone where VAL369 and VAL368 interact with the O atom and the same VAL370 interacts with the OH atom whereas the PRO429 interacts with the NH atom of the ligand

**Table 1.** Showing the docking score and other energy scores generated during the interaction calculations. (Docking and MM\GBSA are in Kcal/mol)

| PDB | Docking Score | MM\ GBSA | Prime Hbond | Prime vdW | mol MW | Ligand efficiency sa | Ligand efficiency In |
|---|---|---|---|---|---|---|---|
| 3EQM | -10.019 | -69.03 | -263.79 | -2269.48 | 434.494 | -3.236 | -15.458 |

### 3.1.3 Molecular and Principle Descriptors of the Ligand:

Several potential therapeutic agents fail during clinical trials due to their unfavourable ADMET properties. ADME calculation is performed to serve the predicted drug-likeness. The calculated ADMET endpoints are summarised in Table 2. The oral availabilities of the compound give the idea of molecular descriptors or properties implicit to drug likeness that work with five descriptors, including molecular weight (MW) ≤ 500 Da, QPlogPo/w value≤ 5, Hydrogen acceptor ≤ 10, Hydrogen donor ≤ 5, Topological Polar Surface Area (TPSA)<5 these criteria follow the Lipinski's rule of five (Lipinski, 2000, 2016). Twenty-two parameters evaluated the pharmacokinetic profile, and most of the values lie within the allowable range. These values are suitable for the selected active ligand. However, the number of likely metabolic reactions also falls within the permissible range. A detailed analysis of molecular dynamics simulation of aromatase protein and the docked structures has been carried out for various parameters. The compound CHEMBL598797 following the binding affinity and Lipinski's rule of five is shown in Table 2.

The logP distribution describes the lipophilicity of a compound that denotes the partition coefficient. The range of hydrogen bond acceptor (HBA) and hydrogen bond donor (HBD) of the compound CHEMBL598797 were 1 and 3.5, respectively, which indicates that the compound denotes a drug-like favourable range. The physiochemical descriptors like SASA, FOSA, FISA, PISA (π component of SASA), QPlogPC16, QPlogPoct, and QPlogPw were also selected for this study, and all parameters were observed within the normal range.

The permeability of the gut-blood barrier predicts by the Caco-2 parameter. It is broadly non-active transport used in blood absorption assay in nm/s (Shin et al., 2016). This parameter helps to identify and evaluate the approximate passage of substances values through the gut wall. The favourable range for the compound CHEMBL598797 was 137.54nm/s, respectively. The QPlogBB partition coefficient is used to predict the compound's brain/blood partition of

bioactive for CNS (Cheng et al., 2013). The scoring range was found to be -0.146 and -2.294. These results show that the top compound was active with the acceptable range in CNS activity. The QPPMDCK is used to predict BBB penetration. The ranges lie between 382.649 and 112.052 nm/sec of the selected drugs. QplogKp calculates the permeability of penetrating the drugs/compounds through the skin. The equation projected the maximum trans-dermal transport rates that symbolise the Jm:

$$Jm = Kp \times MW \times S$$

Jm is the trans-dermal transport rate expressed in the unit of μg cm, Kp symbolises the skin permeability and molecular weight (MW), and S denotes aqueous solubility. The -5.043 (mol dm–3) range was observed in compound CHEMBL598797.

QPlogKhsa has been estimated to predict the plasma-protein binding of the selected compound, which binds to human serum albumin, glycoprotein, globulins, and lipoprotein and has a converse relation to the target obtainability. Drug efficacy is unswervingly influenced by binding ability with the distribution of drugs through the bloodstream and the accessibility of drugs to their target. Consequently, a lower degree of protein bound to plasma is required for designing the drugs. Compound CHEMBL598797 has the following within the suitable range of -0.12 nm/s. QPlogHERG is an essential parameter for predicting blockage of human ether-a-go-go-related gene (hERG) potassium channel for the cardiac and nervous system to predict the cardiac toxicity of druggable molecules (Shahbazi et al., 2016; Thakkar et al., 2017). HERG K+ channels are QPlogKhsa>-5. The channel also has a modulating function in the nervous system. This ADME investigation of CHEMBL598797 displayed that all parameters except CIQPlogS (score 6.6) and QPlogHERG (score 5.9) were favourable values of drug-likeness, metabolism, and pharmacokinetics, criteria.

401 **Table 2.** Showing the QikProp or ADMET result of Ziprasidone
402 (CHEMBL598797) against the standard values
403

| Property or Descriptor | Ziprasidone | QikProp Standard values | Property or Descriptor | QikProp Standard values | Ziprasidone |
|---|---|---|---|---|---|
| #stars | 0 | 0 – 5 | QPlogS | −6.5 – 0.5 | -4.457 |
| #amine | 0 | 0 – 1 | CIQPlogS | −6.5 – 0.5 | -4.96 |
| #amidine | 0 | 0 | QPlogHERG | concern below −5 | -5.395 |
| #acid | 0 | 0 – 1 | QPPCaco | <25 poor, >500 great | 83.169 |
| #amide | 1 | 0 – 1 | QPlogBB | −3.0 – 1.2 | -2.412 |
| #rotor | 13 | 0 – 15 | QPPMDCK | <25 poor, >500 great | 64.628 |
| #rtvFG | 1 | 0 – 2 | QPlogKp | −8.0 −1.0 | -2.765 |
| CNS | -2 | −2 (inactive +2 (active) | IP(eV) | 7.9 – 10.5 | 0 |
| mol MW | 434.494 | 130.0 – 725 | EA(eV) | −0.9 – 1.7 | 0 |
| dipole | 0 | 1.0 – 12.5 | #metab | 1 – 8 | 5 |
| SASA | 804.15 | 300.0 – 1000.0 | QPlogKhsa | −1.5 – 1.5 | -0.123 |
| FOSA | 320.205 | 0.0 – 750.0 | HumanOralAbsorption | N/A | 2 |
| FISA | 191.257 | 7.0 – 330.0 | PercentHumanOralAbsorption | >80% is high, <25% is poor | 77.748 |
| PISA | 292.688 | 0.0 – 450.0 | SAfluorine | 0.0 – 100.0 | 0 |
| WPSA | 0 | 0.0 – 175.0 | SAamideO | 0.0 – 35.0 | 32.947 |
| volume | 1427.933 | 500.0 – 2000.0 | PSA | 7.0 – 200.0 | 117.912 |
| donorHB | 3.5 | 0.0 – 6.0 | #NandO | 2 – 15 | 8 |
| accptHB | 8.2 | 2.0 – 20.0 | RuleOfFive | maximum is 4 | 0 |
| dip^2/V | 0 | 0.0 – 0.13 | RuleOfThree | maximum is 3 | 0 |
| ACxDN^.5/SA | 0.019077 | 0.0 – 0.05 | #ringatoms | N/A | 16 |
| glob | 0.7626058 | 0.75 – 0.95 | #in34 | N/A | 0 |
| QPpolrz | 45.44 | 13.0 – 70.0 | #in56 | N/A | 16 |
| QPlogPC16 | 15.932 | 4.0 – 18.0 | #noncon | N/A | 0 |
| QPlogPoct | 24.48 | 8.0 – 35.0 | #nonHatm | N/A | 32 |
| QPlogPw | 17.72 | 4.0 – 45.0 | Jm | N/A | 0.026 |
| QPlogPo/w | 2.808 | −2.0 – 6.5 | | | |

### 3.1.4 MD Simulation of Protein-Ligand Complex:

The simulation of the docked structure was performed after the equilibration phase for 100 ns and plotted several metrics to prove the stability of the structure. Figure 4 illustrates the atomic contacts between the functional group in the compound CHEMBL598797 and the targeted protein changed during the simulation process. The time course of protein-ligand contacts with intra-atomic distances was not higher than 3.0Å. The targeted peaks were observed, and they can be seen in the saturation binding curve. The region of ligand's RMSD between 23-44ns, 56-66ns and 89-96ns illustrates the periodic higher fluctuations than the other residues because of the conformational switching owing to the hydroxamate and can rotate easily around the atom bonds and interact with water. Finally, it reached the stable RMSD at 2.7 Å. Residues Val369, Val370, Gly439, and Ala438 are significant contributors to the interaction between CHEMBL598797 and aromatase. This result implies stability between the interaction CHEMBL598797 and the targeted protein.

### 3.1.5 Key interaction of ligand and protein:

The best ligand and targeted protein aromatase are essential in strengthening the receptor-ligand interactions, such as hydrogen bonding, hydrophobic interactions, pi cation, and salt bridge, which were visualised. The acceptor hydrogen bond (red) and donor hydrogen bonding (yellow) profiles of co-crystal ligand were close to compound CHEMBL598797. The counts of acceptor and donor remarkably emphasised the significant interaction of hydrogen bonds.

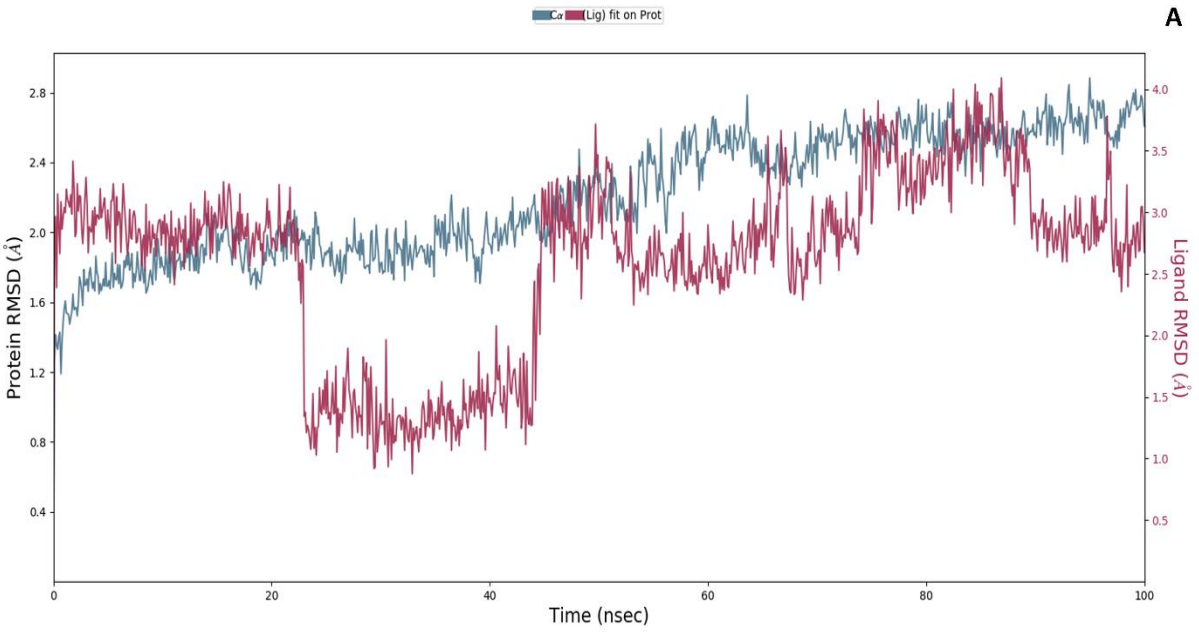


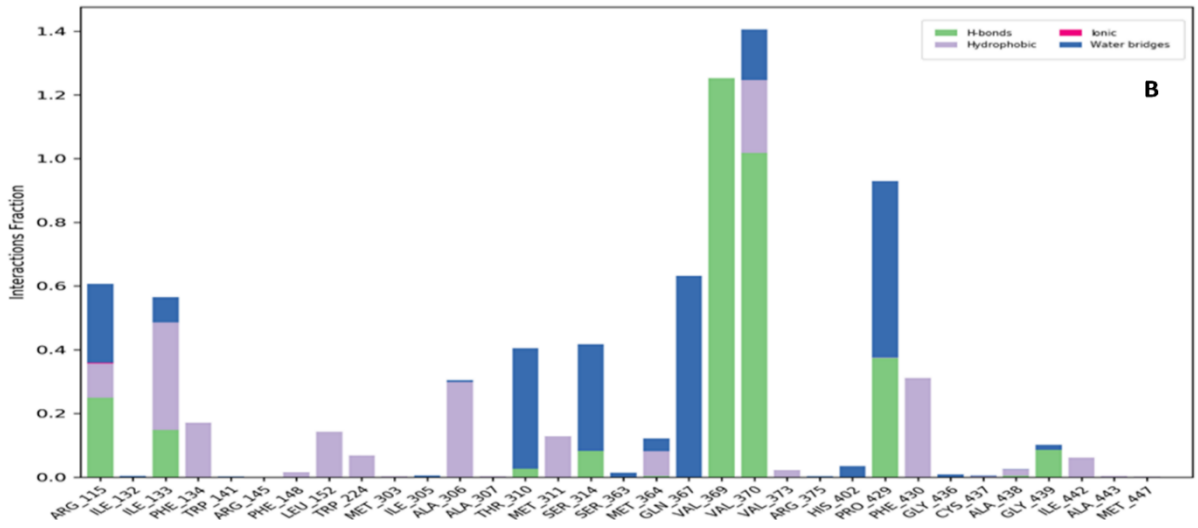


**Figure 3:** Showing the MD Simulation results in **A)** Root Mean Square Deviation (RMSD) and **B)** Histogram representation of Protein-ligand contact number concerning its type in CHEMBL598797 (Ziprasidone)

Figure 4 describes the different intermolecular interactions such as hydrogen bonds, hydrophobic interaction, and water bridge assembled by each pocket residue with ligand binding site. The 2D interaction maps of ChEMBL based docked complex portraying the preservation of contacts through the simulation trajectory are shown in the interaction diagram in Figure 3&4.

Compound ChEMBL598797 depicted the hydrogen bond interaction with the backbone amino acid residues Val369, Val370, Pro429, Ile133, Gln363, Gln367 and Val370 and the side

chain amino acid residues Arg115, Thr310, and Ser 314. Cation π interaction was observed in the residue Arg115, stabilising the electrostatic interaction of a cation of an aromatic ring and four π-π stacking interactions enriched in pi orbital containing between amino acid residues Phe134, Try224, Phe148, and Phe430 and aromatic ring of ziprasidone. These interactions show the involvement of energetic *aromatic amino acid* residues in packing the adenine ring in the targeted protein. Ionic interaction (side chain metal mediate) was also observed in the amino acid residues Arg115 and Arg145. Water bridge (donor) Arg115, Ser314, His402, Arg375, Gly439, Try141. Water bridge (accepter) Ile132, Ile133, Ile305, Ala306, Thr310, Ser363, Met364, Gln367, Val370, Pro429, Gly436.

Compound ChEMBL598797 was efficiently docked and validated for the better quality of the docking results. Some residues displayed a similar hydrogen bonding and hydrophobic interaction with the amino acid residues. The better results prove the ability of the compound to inhibit aromatase target receptors. Figure 4 provides exhaustive binding interactions of the target with selected ligand ChEMBL598797 (Ziprasidone).

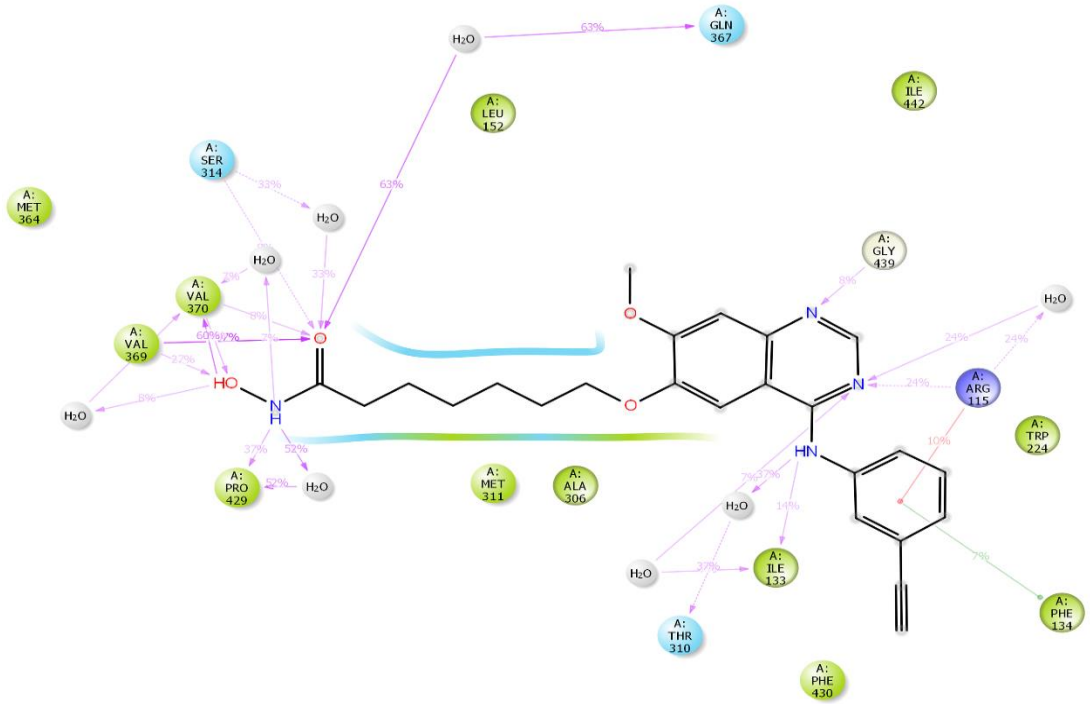


**Figure 4:** Showing 2D protein simulation integration diagram of CHEMBL598797 (Ziprasidone)

### 3.2 *In-vitro* study:

#### 3.2.1 Antiproliferative activity in cancer cells:

The anticancer effect of ziprasidone on the growth of MCF-7, MDA-MB-231 and T47D was detected by MTT as described earlier (Tolosa et al., 2015). In the present experiment, cells were treated with parent compound and these compounds at 2, 1, 0.25, 0.125, and 0.0625 mM for 24 and 48 h. The dose-response curve was used to calculate the $IC_{50}$ value, the drug concentration required to reduce cell proliferation by 50% against an untreated control. The $IC_{50}$ value for Ziprasidone in MCF-7 cells was found to be 0.260 mM and 0.158 mM at 24 and 48 h. For MDA-MB-231 cell lines, the $IC_{50}$ value was 0.532 and 0.27 at 24h and 48 h, respectively (Figure 5). Next, the IC50 values in the case of the T47D cell line were 0.608 at 24 h and 0.336 and 48h. These results showed diminished antiproliferative activity under a similar condition, as seen in Figure 5.

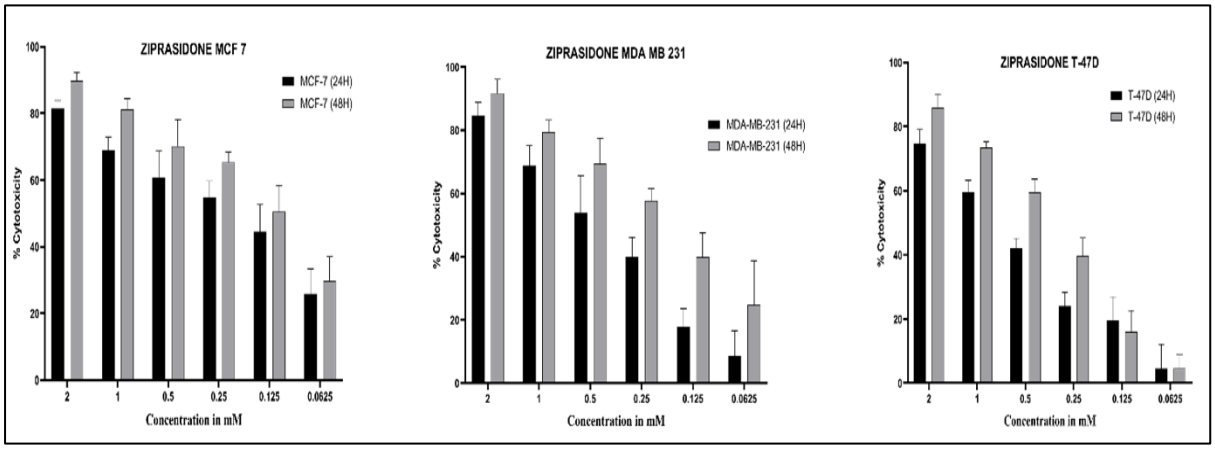


**Figure 5:** Effects of Ziprasidone under antiproliferation activity in MCF-7, MDA MB 231 and T47D cells at 24 and 48h post-treatment

#### 3.2.2 Effects of Ziprasidone on cell Morphology:

Morphological changes were recorded using a microscope in MCF-7, MDA-MB-231 and T47D cells. For all treated cells, the images were observed at 24 h, and the images were captured using a phase-contrast light microscope. Cell in the control group cell shape was not

changed, as in the case of treated groups, there was a substantial change in cell morphology, and cell debris of dead cells was also seen. The treatment with Ziprasidone to MCF 7, MDA MB and T47D cells at different concentrations at 24 h resulted in round shape and size reduction (Figure 6).

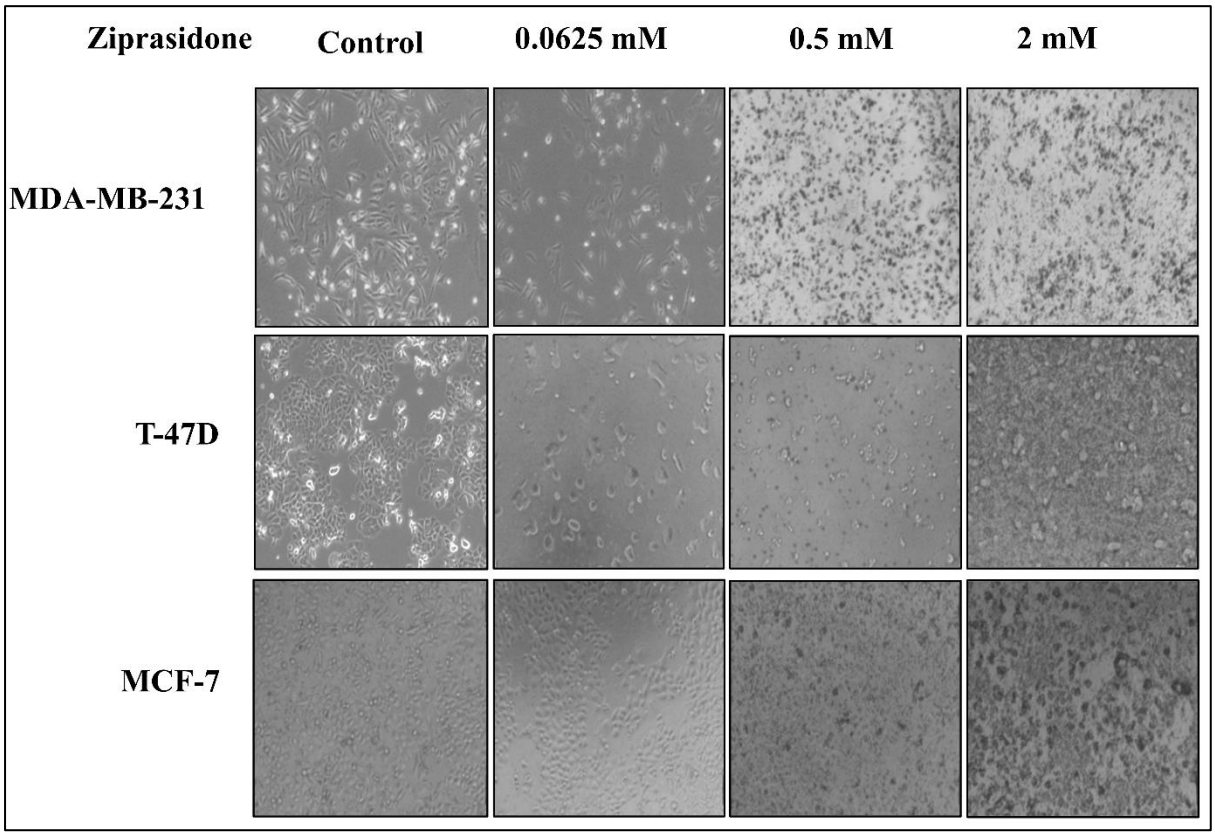


**Figure 6.** Effects of Ziprasidone under study on MCF-7, MDA MB 231 and T47D cells morphology at 24 h post-treatment

### 3.2.3 Cell cycle analysis:

Selected compounds exert growth-inhibitory effects on different cell lines by arresting the cell cycle at a specific phase. The in-vitro screening results in Figure 7 display that ziprasidone significantly increased in the S phase from 8.06% to 12.2% in MCF-7. MDA-MB-231 increased from 9.51% to 12.9% population; furthermore, in case of T47D, it increased from 9.45 % to 13.5 % concerning control.

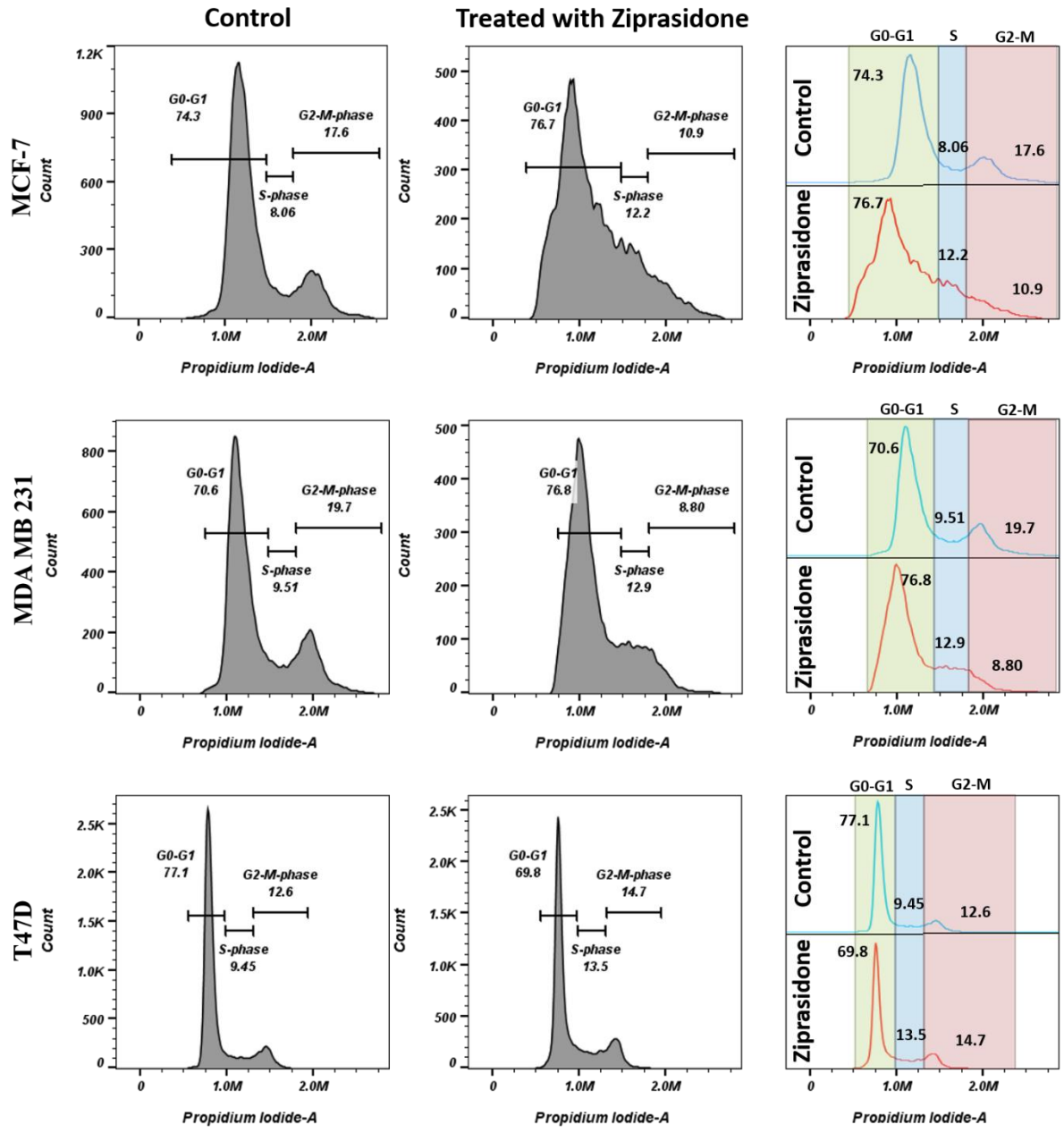


**Figure 7:** Cell cycle analysis in control and treated with drugs with different cell lines (MCF-7, MDAMB 231 and T47D)

### 3.2.4 Annexin V binding assay:

Ziprasidone was further investigated to evaluate their Apoptosis. It is a pathway leading to cell death. To analyse the effect of ziprasidone on the Apoptosis of different cells, we applied FITC-Annexin V and PI double staining for a flow cytometry assay. MCF-7 cells were treated for 24 h with MCF-7, MDA MB 231 and T47D cells and analysed by flow cytometry (Rieger et al., 2011). Figure 8 show an increased cell death ratio between early and late Apoptosis with

increasing concentration of the compound. Remarkably, 2.77% of the cell population underwent the necrotic phase (Q1 quadrant; Figure 8) in all concentrations of ziprasidone treatment. When comparing the early and late apoptosis as well as necrosis phase, the increasing number of cells in the necrotic phase is more pronounced than in the early phase.

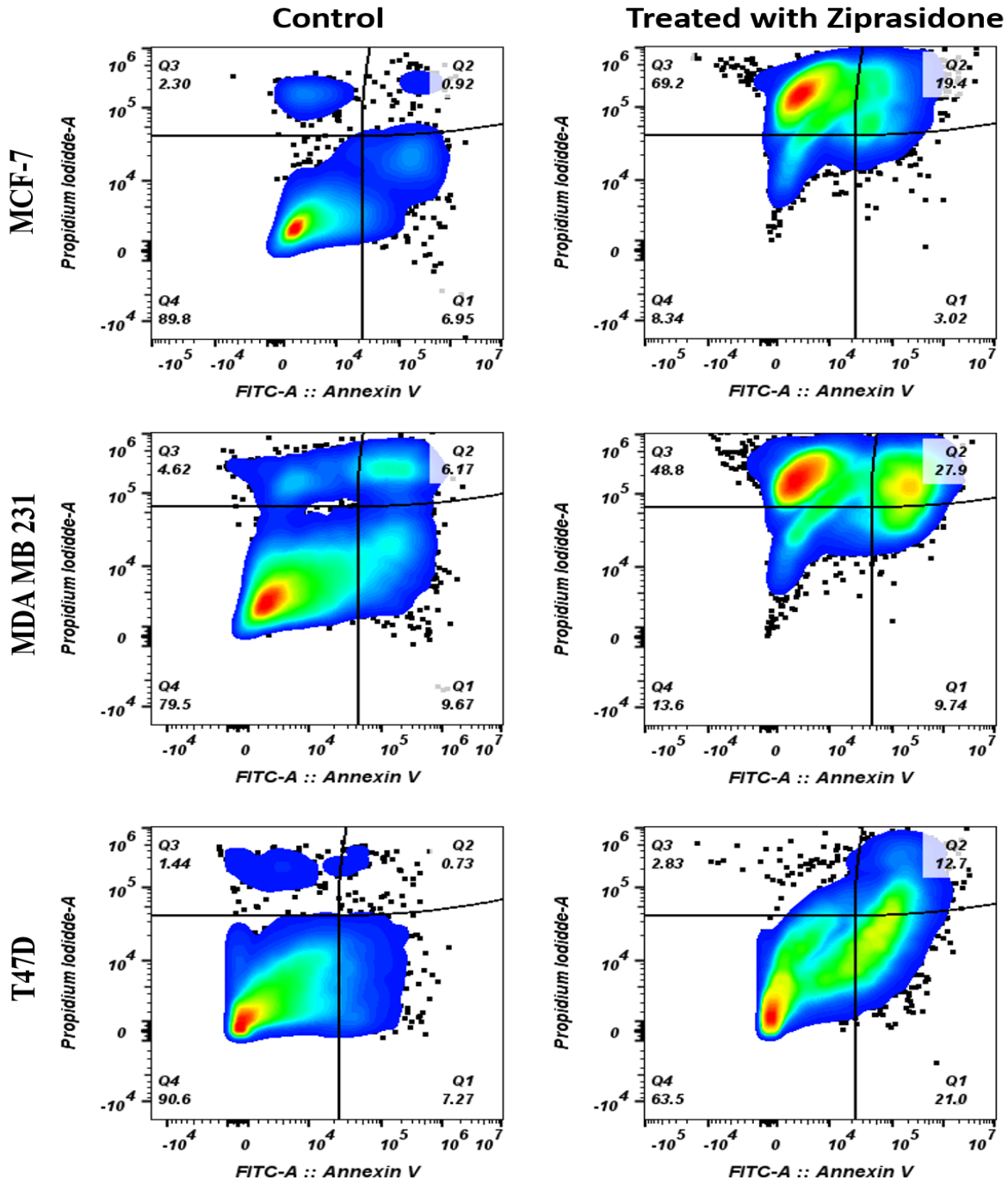


**Figure 8:** The proapoptotic effect of ziprasidone on MCF-7, MDA-MB 231 qnd T47D cell lines after 48h against control and treated cells.

## 4. Discussion:

This study used *in-silico* and *in-vitro* approaches to investigate the particular compound with anticancer effects. Molecular docking approach is considered an emerging field for the rational drug design and development and, therefore, is gaining significance in biomedical science (Shahbazi et al., 2016). Here, computer-aided approaches were adopted to predict whether the selected compound has anticancer potential or not. Aromatase-targeted protein was selected (PDB ID: 3EQM) based on their affiliation with breast cancer. In this study, computer-aided drug design molecular docking indicated that the selected compound (Ziprasidone) interacts with good binding affinities and best binding free energies with aromatase targeted protein at their well-known active sites. Higher positive energies indicate stronger binding, and negative energies indicate the favourable interaction is negative means no binding (Halgren, 2009; Zhang et al., 2017). Therefore, with the help of advanced *in-silico* tools, it was predicted that ziprasidone could work as an anticancer drug agent.

Prediction of anticancer drug potential of ziprasidone through *in-silico* approaches was further validated using *in-vitro* studies. For the *in-vitro* study, MCF-7, MDA MB 231 cells were selected because of their similarities with breast cancer of human origin (Razak et al., 2019). To check the cytotoxic effect of ziprasidone on these cells, the tetrazolium-based MTT assay was performed (Tolosa et al., 2015). MTT is a reliable and sensitive colourimetric technique, which is generally used for measuring *in vitro* cytotoxic effects of drugs on cancer cell lines and assessing the viability and proliferation of cancer cells (Tolosa et al., 2015). Different doses of ziprasidone were selected to determine the most effective dose (ED) or effective concentration (EC) at a minimum concentration. Hence, we started with concentration ranging from 2, 1, 0.25, 0.125, and 0.0625 mM for 24 *in-vitro* studies. Cytotoxic effects of the compound ziprasidone observed using MTT assay on MCF-7, MDA MB 231, and T47D cells indicate dose and time-dependent activities. Our outcomes based on *in-vitro* studies indicate

554 that treatment with ziprasidone causes the death of cancerous in these cells and could act as a
555 cytotoxic agent in concentration and time dependent manner with an $IC_{50}$ value.

556 The ability of a drug to interact with DNA is a significant feature in discovering new
557 anticancer agents. This agent targets the DNA molecule and interfere with the cell cycle leading
558 to cell death. Indeed, DNA interaction alters the cells fate by replication inhibition and/or
559 transcription alteration. Since our finding confirmed the arrest of the cell cycle, ultimately
560 resulting in intrinsic and less likely extrinsic Apoptosis. Since our results confirmed the arrest
561 of cell cycle, ultimately result in the intrinsic and less likely extrinsic apoptosis. To study the
562 inhibitory mode induced by ziprasidone in the MCF-7, MDA-MB-231 and T47D cells cultured,
563 investigated through incubation of cells with AnnexinV-(FITC) and proprium iodide (PI)
564 which confirmed apoptosis in treated cells and it was compatible with the morphological
565 changes of the treated cells under the microscope. On the whole, our findings of this study
566 suggest that compound ziprasidone has been recognized as potential anticancer agent.

567 **5. Conclusion:**

568 The noteworthy conclusion is to find the remarkable agents for the aromatase target. The top
569 compound CHEMBL598797 had better binding affinities based on the docking score. Toxicity
570 and ADMET properties were predicted using computational calculations. The finding of this
571 study suggests that this compound could be a potent inhibitor for the aromatase target. The
572 efficiency of the selected compound will further be confirmed based on wet-lab experiments.
573 The computational pipelines mentioned in this study would be beneficial in predicting possible
574 potent inhibitors for the aromatase enzyme for breast cancer treatment. The cytotoxic results
575 of this ziprasidone compound confirm it as a chemotherapeutic agent. This compound was
576 tested for its capability to induce cell cycle arrest and apoptosis in MCF-7, MDA MB 231 and
577 T47D breast cancer cells. In conclusion, ziprasidone, from screening in-silico molecular

docking tools and in-vitro anticancer evaluation studies, emerged as a potential lead anticancer candidate for breast cancer.

**Acknowledgement:** The authors would like to thank Dr. Nirupama Trihanpati (Institute of Liver and Biliary Sciences) for providing the lab facilities for experimental work. We also thanks Mr. Nagarjuna A Tirunelvely for helpful discussions in the flowcytometry.

**Funding statement:** The Indian Council of Medical Research (ICMR) supported this work under Grant 45/17/2019-BMS/PHA.

**Data availability statement:** The data that support the findings of this study are available from the corresponding author upon reasonable request. Some data may not be made available because of privacy or ethical restrictions.

**Competing interests:** None of the authors has any conflict of interests.

**Author contribution statement:** AS (first author) collected data from literature and database; performed computational studies and writing the manuscript; SA Performed the molecular dynamics experiment and helped in the writing of in-silico studies, and edited the manuscript; ME Provided the molecular modelling lab facility; KI Performed the in-vitro studies; SV helped in writing manuscript, suggested methodology and plan, discussion on all aspects with overall supervision of results; KR Conducted planning of computational work, verified computational results and discussion; ME and MAR provided suggestions and helped with manuscript editing. All authors read and approved the final manuscript.

**References:**

Adcock, S.A., and McCammon, J.A. (2006). Molecular dynamics: survey of methods for simulating the activity of proteins. Chem Rev *106*: 1589–1615.

Alonso, H., Bliznyuk, A.A., and Gready, J.E. (2006). Combining docking and molecular dynamic simulations in drug design. Med Res Rev *26*: 531–568.

Altundag, K., and Ibrahim, N.K. (2006). Aromatase inhibitors in breast cancer: an overview. Oncologist *11*: 553–562.

Anthoni, H., Sucheston, L.E., Lewis, B.A., Tapia-Páez, I., Fan, X., Zucchelli, M., et al. (2012). The Aromatase Gene CYP19A1: Several Genetic and Functional Lines of Evidence Supporting a Role in Reading, Speech and Language. Behav Genet *42*: 509–527.

Appert-Collin, A., Hubert, P., Crémel, G., and Bennasroune, A. (2015). Role of ErbB Receptors in Cancer Cell Migration and Invasion. Front Pharmacol *6*: 283.

Arora, A., and Scholar, E.M. (2005). Role of tyrosine kinase inhibitors in cancer therapy. J. Pharmacol. Exp. Ther. *315*: 971–979.

Atalay, G., Cardoso, F., Awada, A., and Piccart, M.J. (2003). Novel therapeutic strategies targeting the epidermal growth factor receptor (EGFR) family and its downstream effectors in breast cancer. Ann. Oncol. *14*: 1346–1363.

Berman, H.M., Westbrook, J., Feng, Z., Gilliland, G., Bhat, T.N., Weissig, H., et al. (2000). The Protein Data Bank. Nucleic Acids Res *28*: 235–242.

Cava, C., and Castiglioni, I. (2020). Integration of Molecular Docking and In Vitro Studies: A Powerful Approach for Drug Discovery in Breast Cancer. Applied Sciences *10*: 6981.

Chan, H.J., Petrossian, K., and Chen, S. (2016). Structural and Functional Characterization of Aromatase, Estrogen Receptor, and Their Genes in Endocrine-Responsive and – Resistant Breast Cancer Cells. J Steroid Biochem Mol Biol *161*: 73–83.

Cheng, F., Li, W., Liu, G., and Tang, Y. (2013). In silico ADMET prediction: recent advances, current challenges and future trends. Curr Top Med Chem *13*: 1273–1289.

Czajka-Oraniec, I., and Simpson, E.R. (2010). Aromatase research and its clinical significance. Endokrynol Pol *61*: 126–134.

Dasari, T., Kondagari, B., Dulapalli, R., Abdelmonsef, A.H., Mukkera, T., Padmarao, L.S., et al. (2017). Design of novel lead molecules against RhoG protein as cancer target – a computational study. Journal of Biomolecular Structure and Dynamics *35*: 3119–3139.

Davies, M., Nowotka, M., Papadatos, G., Dedman, N., Gaulton, A., Atkinson, F., et al. (2015). ChEMBL web services: streamlining access to drug discovery data and utilities. Nucleic Acids Research *43*: W612–W620.

Egan, W.J., and Lauri, G. (2002). Prediction of intestinal permeability. Adv Drug Deliv Rev *54*: 273–289.

Elokely, K.M., and Doerksen, R.J. (2013). Docking challenge: Protein sampling and molecular docking performance. J Chem Inf Model *53*: 1934–1945.

Ferreira, L.G., Dos Santos, R.N., Oliva, G., and Andricopulo, A.D. (2015). Molecular Docking and Structure-Based Drug Design Strategies. Molecules *20*: 13384–13421.

Friesner, R.A., Banks, J.L., Murphy, R.B., Halgren, T.A., Klicic, J.J., Mainz, D.T., et al. (2004). Glide: a new approach for rapid, accurate docking and scoring. 1. Method and assessment of docking accuracy. J. Med. Chem. *47*: 1739–1749.

Friesner, R.A., Murphy, R.B., Repasky, M.P., Frye, L.L., Greenwood, J.R., Halgren, T.A., et al. (2006). Extra precision glide: docking and scoring incorporating a model of hydrophobic enclosure for protein-ligand complexes. J. Med. Chem. *49*: 6177–6196.

Gaulton, A., Bellis, L.J., Bento, A.P., Chambers, J., Davies, M., Hersey, A., et al. (2012). ChEMBL: a large-scale bioactivity database for drug discovery. Nucleic Acids Res *40*: D1100–D1107.

Genheden, S., and Ryde, U. (2015). The MM/PBSA and MM/GBSA methods to estimate ligand-binding affinities. Expert Opin Drug Discov *10*: 449–461.

Ghosh, D., Griswold, J., Erman, M., and Pangborn, W. (2010). X-ray Structure of Human Aromatase Reveals An Androgen-Specific Active Site. J Steroid Biochem Mol Biol *118*: 197–202.

Halgren, T.A. (2009). Identifying and characterizing binding sites and assessing druggability. J Chem Inf Model *49*: 377–389.

Karplus, M., and McCammon, J.A. (2002). Molecular dynamics simulations of biomolecules. Nat. Struct. Biol. *9*: 646–652.

Kumavath, R., Azad, M., Devarapalli, P., Tiwari, S., Kar, S., Barh, D., et al. (2016). Novel aromatase inhibitors selection using induced fit docking and extra precision methods: Potential clinical use in ER-alpha-positive breast cancer. Bioinformation *12*: 324–331.

Laskowski, R.A., MacArthur, M.W., Moss, D.S., and Thornton, J.M. (1993). PROCHECK: a program to check the stereochemical quality of protein structures. J Appl Cryst *26*: 283–291.

Lephart, E.D. (2015). Modulation of Aromatase by Phytoestrogens. Enzyme Research *2015*: e594656.

Lipinski, C.A. (2000). Drug-like properties and the causes of poor solubility and poor permeability. J Pharmacol Toxicol Methods *44*: 235–249.

Lipinski, C.A. (2016). Rule of five in 2015 and beyond: Target and ligand structural limitations, ligand chemistry structure and drug discovery project decisions. Adv. Drug Deliv. Rev. *101*: 34–41.

Michels, K.B. (2002). The contribution of the environment (especially diet) to breast cancer risk. Breast Cancer Research *4*: 58.

Mori, T., Ito, F., Koshiba, A., Kataoka, H., Tanaka, Y., Okimura, H., et al. (2018). Aromatase as a target for treating endometriosis. Journal of Obstetrics and Gynaecology Research *44*: 1673–1681.

Nelson, L.R., and Bulun, S.E. (2001). Estrogen production and action. J Am Acad Dermatol *45*: S116-124.

Norinder, U., and Bergström, C.A.S. (2006). Prediction of ADMET Properties. ChemMedChem *1*: 920–937.

Ntie-Kang, F. (2013). An in silico evaluation of the ADMET profile of the StreptomeDB database. Springerplus *2*:.

Paul, S.M., Mytelka, D.S., Dunwiddie, C.T., Persinger, C.C., Munos, B.H., Lindborg, S.R., et al. (2010). How to improve R&D productivity: the pharmaceutical industry's grand challenge. Nat Rev Drug Discov *9*: 203–214.

Rana, M., Arif, R., Khan, F.I., Maurya, V., Singh, R., Faizan, M.I., et al. (2021). Pyrazoline analogs as potential anticancer agents and their apoptosis, molecular docking, MD simulation, DNA binding and antioxidant studies. Bioorganic Chemistry *108*: 104665.

Razak, N.A., Abu, N., Ho, W.Y., Zamberi, N.R., Tan, S.W., Alitheen, N.B., et al. (2019). Cytotoxicity of eupatorin in MCF-7 and MDA-MB-231 human breast cancer cells via cell cycle arrest, anti-angiogenesis and induction of apoptosis. Scientific Reports *9*: 1514.

Rieger, A.M., Nelson, K.L., Konowalchuk, J.D., and Barreda, D.R. (2011). Modified Annexin V/Propidium Iodide Apoptosis Assay For Accurate Assessment of Cell Death. J Vis Exp 2597.

Sahu, A., Patra, P.K., Yadav, M.K., and Varma, M. (2017). Identification and characterization of ErbB4 kinase inhibitors for effective breast cancer therapy. J. Recept. Signal Transduct. Res. *37*: 470–480.

Sahu, A., Pradhan, D., Raza, K., Qazi, S., Jain, A. K., & Verma, S. (2020). In silico library design, screening and MD simulation of COX-2 inhibitors for anticancer activity. *BICOB (EPiC Series in Computing)*, 70, 21–32.

Santen, R.J., Brodie, H., Simpson, E.R., Siiteri, P.K., and Brodie, A. (2009). History of Aromatase: Saga of an Important Biological Mediator and Therapeutic Target. Endocr Rev *30*: 343–375.

Sastry, G.M., Adzhigirey, M., Day, T., Annabhimoju, R., and Sherman, W. (2013). Protein and ligand preparation: parameters, protocols, and influence on virtual screening enrichments. J Comput Aided Mol Des *27*: 221–234.

Shahbazi, S., Sahrawat, T.R., Ray, M., Dash, S., Kar, D., and Singh, S. (2016). Drug Targets for Cardiovascular-Safe Anti-Inflammatory: In Silico Rational Drug Studies. PLoS One *11*:.

Shaheenah, D., Fellow, S.G.K., and Buzdar, A.U. (2008). Aromatase. In Encyclopedia of Molecular Pharmacology, S. Offermanns, and W. Rosenthal, eds. (Berlin, Heidelberg: Springer), pp 218–221.

Shin, H.K., Kang, Y.-M., and No, K.T. (2016). Predicting ADME Properties of Chemicals. In Handbook of Computational Chemistry, J. Leszczynski, ed. (Dordrecht: Springer Netherlands), pp 1–37.

Smith, I.E., and Dowsett, M. (2003). Aromatase inhibitors in breast cancer. N Engl J Med *348*: 2431–2442.

Thakkar, S.S., Thakor, P., Doshi, H., and Ray, A. (2017). 1,2,4-Triazole and 1,3,4-oxadiazole analogues: Synthesis, MO studies, in silico molecular docking studies, antimalarial as DHFR inhibitor and antimicrobial activities. Bioorg Med Chem *25*: 4064–4075.

Tolosa, L., Donato, M.T., and Gómez-Lechón, M.J. (2015). General Cytotoxicity Assessment by Means of the MTT Assay. Methods Mol Biol *1250*: 333–348.

Torres, P.H.M., Sodero, A.C.R., Jofily, P., and Silva-Jr, F.P. (2019). Key Topics in Molecular Docking for Drug Design. Int J Mol Sci *20*:.

Travis, R.C., and Key, T.J. (2003). Oestrogen exposure and breast cancer risk. Breast Cancer Research : BCR *5*: 239.

Wang, E., Sun, H., Wang, J., Wang, Z., Liu, H., Zhang, J.Z.H., et al. (2019). End-Point Binding Free Energy Calculation with MM/PBSA and MM/GBSA: Strategies and Applications in Drug Design. Chem. Rev. *119*: 9478–9508.

Zhang, X., Perez-Sanchez, H., and Lightstone, F.C. (2017). A Comprehensive Docking and MM/GBSA Rescoring Study of Ligand Recognition upon Binding Antithrombin. Curr Top Med Chem *17*: 1631–1639.